

SILICON CARBIDE MEMS OSCILATOR

*İ. Engin Pehlivanoğlu, Christian A. Zorman, and Darrin J. Young**

Electrical Engineering and Computer Science Department
Case Western Reserve University, Cleveland, Ohio, USA

ABSTRACT

An oscillator employing a polycrystalline 3C silicon carbide (3C-SiC) folded-beam microelectromechanical resonator as a frequency-setting component with silicon discrete electronics has been designed and demonstrated. The rocking resonant mode of the resonator is chosen due to its lower motional resistance than that of the lateral resonant mode and small frequency separation between the two modes. Further analysis reveals that an increased power handling capability can be obtained by the rocking mode without an excessive mechanical motion, which is attractive for enhancing resonator durability. The resonator achieves a quality factor of 10300 at 30.2 kHz of the rocking mode resonance under 1 mTorr pressure. The oscillator outputs a sinusoidal waveform at 30.2 kHz with an output power of -17 dBm under a 10V DC bias and achieves a phase noise of -78 dBc/Hz at 12 Hz offset frequency from the carrier, limited by the resonator power handling capability and noise floor from the interface electronics. The oscillation frequency exhibits a 16 ppm stability observed over a period of 100 hours including all environment effects.

KEYWORDS

MEMS Oscillator, Silicon Carbide MEMS, MEMS Resonator.

INTRODUCTION

Harsh environment sensing, signal processing, and wireless data transmission are critical for advanced industrial, automotive and aerospace applications. Typical temperatures for these applications range from 200 °C to 600 °C. Higher temperatures up to and beyond 1000 °C are required for extreme harsh environments such as turbine engines and nuclear power generators. In a practical sensing system, a time-stable reference clock is required for timing synchronization and frequency translation. Conventional quartz crystals and, recently, silicon MEMS resonators have been employed for generating such references [1, 2]. These frequency-setting components, however, suffer from degraded performance at elevated temperatures. It has been shown that SiC can serve as a critical material for implementing high-temperature MEMS devices [3]. SiC-based pressure sensors and strain sensors have been demonstrated for high temperature sensing applications [4, 5, 6, 7, 8]. Research effort was also devoted to develop single crystal 6H-SiC MEMS fabrication process based on proton-implantation

and smart-cut technique for potential monolithic integration of SiC MEMS devices and microelectronics [9]. In this paper, an oscillator employing a polycrystalline 3C silicon carbide folded-beam microelectromechanical resonator as a frequency-setting component with silicon discrete electronics is presented. The folded-beam resonator, instead of other more complex resonator topologies, is chosen to determine the oscillator steady-state oscillation frequency due to its robust design and one-mask fabrication simplicity. An adequate power handling capability can be obtained in the rocking resonant mode of the resonator, compared to the lateral resonant mode, without an excessive mechanical motion, thus attractive for enhancing resonator durability. The research findings from the 3C-SiC resonator are applicable to other folded-beam resonators design fabricated in all types of SiC material.

3C SILICON CARBIDE MEMS RESONATOR

The 3C-SiC MEMS resonator employed in the prototype oscillator design was fabricated in a single-mask surface-micromachined silicon carbide MEMS fabrication process [10]. Figure 1 presents an SEM photo of a fabricated folded-beam MEMS resonator. The device exhibits a folded-beam suspension length of 154 μm with a width of 2.4 μm , comb finger width of 5 μm with a gap size of 2 μm , and a proof mass of 0.14 micro-gram (μg). This resonator configuration is chosen because the probe pads can be positioned around the device for convenient electrical connections due to the single-mask fabrication process.

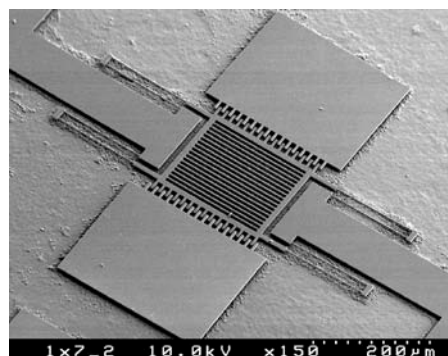


Figure 1: SEM of fabricated 3C-SiC MEMS resonator

ANALYSIS AND CHARACTERIZATION OF MEMS RESONATOR

Electromechanical analysis reveals that the prototype MEMS resonator exhibits three modes of resonance: (1)

lateral mode where the motion of the proof mass is parallel to the substrate, (2) vertical mode where the proof mass vibrates up and down with respect to the substrate, and (3) rocking mode where the rotational vibration of the proof mass is along the device centerline parallel to the suspensions. Based on the fabricated resonator dimensions, the resonant frequency of the lateral, rocking, and vertical modes is calculated as 30.9 kHz, 31.6 kHz, and 25.8 kHz, respectively. Finite element simulation reveals the corresponding resonances at 28.7 kHz, 34.4 kHz, and 26.2 kHz. It is noted that the three resonant modes are close to each other in terms of frequency separation. To further investigate the resonant behavior, the prototype SiC resonator is characterized for its magnitude and phase frequency response. Figure 2 presents the measured frequency response of the resonator under 10V DC bias and 1 mTorr pressure, indicating the lateral resonance of 27.1 kHz, rocking resonance of 30.3 kHz, and vertical resonance of 24.2 kHz, with the corresponding phase shift between the output motional current and input excitation voltage of 0° , 0° , and 180° , respectively. Zoom-in analysis of the frequency response shows an achieved Q value of 13550, 10300, and 9480 for the lateral, rocking and vertical modes, respectively. In a typical capacitive-based resonator design, the lateral resonant mode is preferred over the vertical mode due to the reduced air damping and large obtainable linear motion with respect to the excitation voltage. For the prototype resonator it is inevitable to excite the lateral mode without exciting the rocking mode because the rocking mode exhibits a higher gain than that of the lateral mode, a small frequency separation from the lateral resonance, and the same phase shift as the lateral resonance. However, a closed-loop oscillator design with a proper small-signal loop gain can ensure the excitation of the rocking resonant mode as the only resonance.

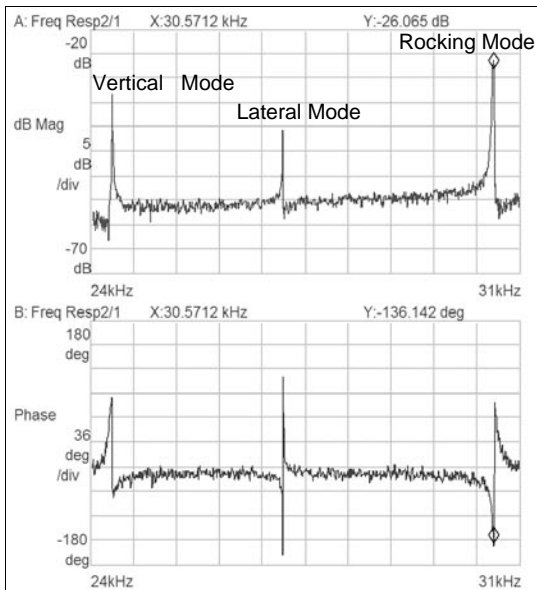


Figure 2: Magnitude and phase frequency response

One of the important performance metrics of an oscillator is the output power or power handling capability because a large output power can result in a low phase noise, thus an improved frequency stability. The output power of a MEMS resonator is commonly characterized by the output current with its magnitude expressed by Equation (1),

$$i = V_{dc-s} \omega x_{ac} \frac{\partial C_s}{\partial x} \quad (1)$$

where V_{dc-s} is the DC bias voltage over the sense-port, ω is the angular frequency, x_{ac} is the vibration displacement amplitude, and $\frac{\partial C_s}{\partial x}$ is the derivative of sensor port capacitance with respect to position along the resonant vibration direction. In a practical application, V_{dc-s} is limited by the system power supply, and ω is determined by application specifications. Therefore, increasing $x_{ac} \frac{\partial C_s}{\partial x}$, the displacement amplitude multiplied by sense-port capacitance change with respect to position, is an effective means to enhance output signal current. In the lateral mode, the capacitance change with respect to displacement excluding fringing filed effect can be expressed as

$$\frac{\partial C}{\partial x} = \frac{\epsilon_0 h}{g}, \quad (2)$$

where h is the finger thickness and g is the gap size between the fingers as depicted in Figure 3. This term will diminish when the vibration amplitude approaches to the fingers overlap length of l . Therefore, a maximum value of $x_{ac} \frac{\partial C}{\partial x}$ can be estimated as $l \frac{\epsilon_0 h}{g}$.

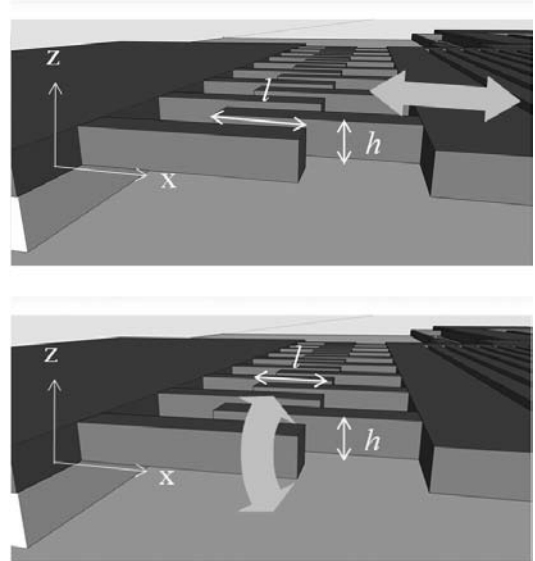


Figure 3: Fingers capacitive coupling in lateral mode (top) and rocking mode (bottom)

Similar applies in the rocking mode, assuming a small angle of rotation the capacitance change with respect to displacement excluding fringing filed effect can be expressed as

$$\frac{\partial C}{\partial z} = \frac{\epsilon_0 l}{g}. \quad (3)$$

Thus, with a maximum vertical tilting displacement of h , $z_{ac} \frac{\partial C}{\partial z}$ will be maximized approximately at $h \frac{\epsilon_0 l}{g}$.

Therefore, both the lateral and rocking modes can produce a comparable maximum output signal current. In order to increase the output current, the fingers overlap length of l and thickness of h should be increased, whereas the gap size, g , between the fingers needs to be reduced. The structural thickness and minimum gap size are limited by the fabrication technology. Therefore, the only design parameter for increasing output signal current is the fingers overlap length. Increasing the fingers overlap length in a lateral mode resonator will call for an increased device area due to the large resulting mechanical motion. The large motion would potentially cause a more pronounced mechanical fatigue, thus a reduced lifespan of the resonator. However, in the rocking mode increasing fingers overlap length does not necessitate an increased lateral motion; hence the device area. The resonator can still achieve an increased output signal current with the same amount of the vertical tilting displacement, which represents an important advantage over the lateral mode resonator. This feature is particularly critical for surface-micromachined SiC folded-beam resonators exhibiting a structural thickness of a few micrometers. A rocking mode resonator with a much improved power handling capability thus can be designed in the future with an extended fingers overlap length compared to the prototype resonator exhibiting an overlap length of $5 \mu\text{m}$.

The nonlinearity of the resonator transfer function at its rocking mode resonance is characterized with an AC input voltage driving the resonator at its resonant frequency. The output current from the resonator sensor-port is recorded as a function of the input driving voltage amplitude. The ratio of the input driving voltage amplitude and the output current amplitude is defined as the resonator motional resistance. Figure 4 presents the measured motional resistance versus AC input driving voltage amplitude under a 10V DC bias and 1 mTorr pressure, indicating an increased motional resistance or a corresponding decreased output current as the input driving voltage amplitude increases.

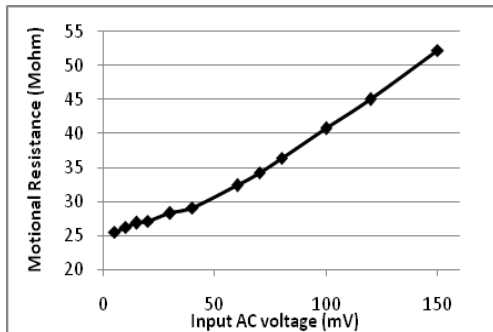


Figure 4: Motional resistance vs. input voltage amplitude

The nonlinearity of the resonator together with the oscillator small-signal loop gain is important for determining the steady-state oscillation amplitude, thus the output signal power as will be illustrated in the following section.

OSCILLATOR DESIGN

The oscillator design consists of the MEMS resonator as the frequency-setting component and electronic amplification stages to ensure an adequate small-signal loop gain with a total loop phase shift of 0° at the desired oscillation frequency. Figure 5 presents the oscillator design topology, where two inverting electronic amplification stages are employed to ensure the required total loop phase shift of 0° at the rocking resonance. Silicon electronics are used for the prototype oscillator evaluation at room temperature. SiC interface electronics will be designed as the next step to achieve higher temperature performance.

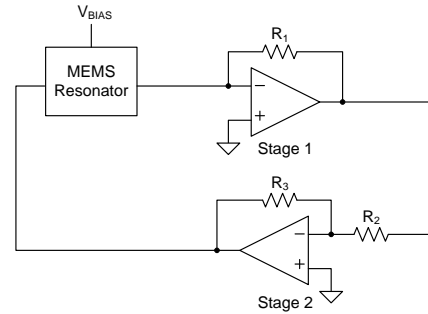


Figure 5: MEMS-resonator-based oscillator design topology

It is noted that the corresponding resonator motional resistance with a small-signal driving voltage is approximately $25 \text{ M}\Omega$ under 10V DC bias and 1 mTorr pressure. Furthermore, a 12 dB magnitude difference between the lateral mode and rocking mode shown in Figure 2 indicates the resonator motional resistance of approximately $98 \text{ M}\Omega$ at the lateral resonance under the same operating condition. Therefore, an electronic amplification system with a gain of 152 dB is designed to achieve a small-signal loop gain of 4 dB at the rocking resonance and -8 dB at the lateral resonance, thus ensuring a reliable oscillation start up and a steady-state oscillation set by the resonator rocking mode resonance. Based on the resonator nonlinearity illustrated in Figure 4, a steady-state oscillation amplitude of approximately 80 mV is expected at the drive-port of the resonator, because this level of input excitation would cause an increased resonator motional resistance of $40 \text{ M}\Omega$; hence, a closed-loop gain of unity for reaching a steady-state operation.

Besides designing the proper small-signal loop gain and total loop phase shift of 0° to ensure a reliable oscillation start up, the electronic noise from the 1st-stage amplifier is critical for achieving a low phase noise performance. To make a quantitative analysis, a term of signal-to-noise-floor ratio (SN_fR) is defined as the ultimate

phase noise achievable from the oscillator and can be expressed as

$$SNfR = \left| \frac{V_{out_signal}}{V_{out_noise_floor}} \right|, \quad (4)$$

where V_{out_signal} is the RMS voltage amplitude at the 1st-stage amplifier output, and $V_{out_noise_floor}$ is the corresponding output noise floor. With a low noise amplifier employed to implement the 1st-stage trans-impedance amplifier, the output electronic noise floor is dominated by the thermal noise of the feedback resistor, R_1 . Thus, $SNfR$ can be further expressed as

$$SNfR = \frac{I_{in}}{\sqrt{2}} \sqrt{\frac{R_1}{4kT}} \quad (5)$$

where I_{in} is the resonator output signal current amplitude. It can be seen that increasing R_1 would result in an improved $SNfR$. However, due to the parasitic capacitance at the input of the trans-impedance amplifier, the feedback resistor, R_1 , cannot be arbitrarily large for ensuring the amplifier stability. R_1 of 1 M Ω is chosen for the prototype design. With a steady-state voltage amplitude of 80mV at the resonator drive-port and a motional resistance of 40 M Ω , the resonator output current amplitude of 2nA is expected. Therefore, an $SNfR$ of 80 dB/Hz can be achieved, which corresponds to an ultimate phase noise of -80 dBc/Hz achievable from the prototype oscillator.

MEASUREMENT RESULTS

Figure 6 presents the measured oscillator output power spectrum indicating a desired oscillation frequency of 30.24 kHz with -17 dBm power. The corresponding time domain waveform with an amplitude of 50mV is shown in Figure 7. The oscillator achieves a minimum phase noise of -78 dBc/Hz at 12 Hz offset frequency, limited by the available signal power and system electronic noise floor. Frequency stability tested over 100 hours at room temperature under 1 mTorr pressure demonstrates that the oscillation frequency deviates from its nominal value by less than 0.5 Hz, corresponding to 16 ppm change including all environmental effects.

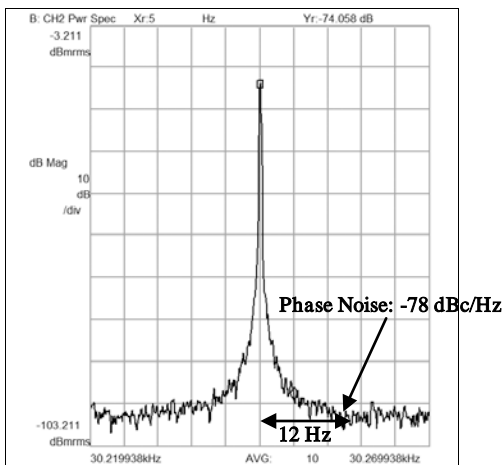


Figure 6: Oscillator output power spectrum

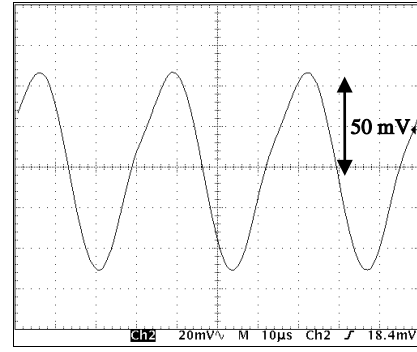


Figure 7: Time domain oscillator output waveform

CONCLUSION

An oscillator employing a polycrystalline 3C silicon carbide folded-beam microelectromechanical resonator as a frequency-setting component with silicon discrete electronics has been designed and demonstrated. The rocking resonant mode of the resonator is chosen due to its lower motional resistance than that of the lateral resonant mode and small frequency separation between the two modes. Further analysis reveals that an increased power handling capability can be obtained by the rocking mode without an excessive mechanical motion, which is attractive for enhancing resonator durability. The resonator achieves a quality factor of 10300 at 30.2 kHz of resonance under 1 mTorr pressure. The oscillator outputs a sinusoidal waveform at 30.2 kHz with an output power of -17 dBm under a 10V DC bias and achieves a phase noise of -78 dBc/Hz at 12 Hz offset frequency from the carrier.

REFERENCES

- [1] J. Salvia, *et al*, "Exploring the Limits and Practicality of Q-based Temperature Compensation for Silicon Resonators," *IEDM*, December 2008.
- [2] M. Mehregany, C. A. Zorman, N. Rajan, and C. H. Wu, "Silicon Carbide MEMS for Harsh Environments," *Proc. IEEE*, vol. 86, August 1998, pp. 1594-1610.
- [3] D. J. Young, J. Du, C. A. Zorman, W. H. Ko, "High-Temperature Single Crystal 3C-SiC Capacitive Pressure Sensor," *IEEE Sensors Journal*, August, pp. 464-470, 2004.
- [4] R. G. Azevedo, *et al*, "A SiC MEMS Resonant Strain Sensor for Harsh Environment Applications," *IEEE Sensors Journal*, Vol. 7, No. 4, pp. 568-576, 2007.
- [5] J. Trevino, *et al*, "Low-stress, heavily-doped polycrystalline silicon carbide for MEMS applications," *MEMS*, 2005, pp. 451-454.
- [6] P. Cong and D. J. Young, "Single Crystal 6H-SiC MEMS Fabrication Based On Smart-Cut Technique," *Journal of Micromechanics and Microengineering*, pp. 2243-2248, 2005.

CONTACT

*Darrin J. Young, darrin.young@case.edu